EKSPLOATACJA I NIEZAWODNOŚĆ MAINTENANCE AND RELIABILITY

Eksploatacja i Niezawodnosc – Maintenance and Reliability

Volume 23 (2021), Issue 1

journal homepage: http://www.ein.org.pl

Article citation info:
Knypiński Ł. Constrained optimization of line-start PM motor based on the gray wolf optimizer. Eksploatacja i Niezawodnosc – Maintenance and Reliability 2021; 23 (1): 1–10, http://dx.doi.org/10.17531/ein.2021.1.1.

Constrained optimization of line-start PM motor based on the gray wolf optimizer

Indexed by: Web of Science Group

Łukasz Knypiński[a]

[a]Institute of Electrical Engineering and Electronics, Faculty of Control, Robotics and Electrical Engineering, Poznan University of Technology, ul. Piotrowo 3A, 60-965 Poznań, Poland

Highlights

- Constrained optimization procedure for the line-start permanent magnet motor.
- The mathematical model of designed motor was developed on the basis of Finite Element Method (FEM).
- The objective function contains product of multiplication of three maintenance parameters of the motor.
- The performance reliability of three heuristic algorithm was compared, i.e. (a) GWO, (b) PSO, (c) BA and (d) GA.

Abstract

This paper presents the algorithm and computer software for constrained optimization based on the gray wolf algorithm. The gray wolf algorithm was combined with the external penalty function approach. The optimization procedure was developed using Borland Delphi 7.0. The developed procedure was then applied to design of a line-start PM synchronous motor. The motor was described by three design variables which determine the rotor structure. The multiplicative compromise function consisted of three maintenance parameters of designed motor and one non-linear constraint function was proposed. Next, the result obtained for the developed procedure (together with the gray wolf algorithm) was compared with results obtained using: (a) the particle swarm optimization algorithm, (b) the bat algorithm and (c) the genetic algorithm. The developed optimization algorithm is characterized by good convergence, robustness and reliability. Selected results of the computer simulation are presented and discussed.

Keywords

heuristic algorithms, gray wolf algorithm, constrained optimization, external penalty function, line-start PM synchronous motor.

Nomenclature:

A_k, C_k – factors of the gray wolf algorithm,
$\mathbf{X}_{k\text{-}1}^{p}$ – vector of the location of the prey,
r, r_1, r_2, κ – random numbers from range (0, 1),
b_k – coefficient describing the ability of migration of wolfs,
$\mathbf{X}_{k\text{-}1}^{\alpha}$, $\mathbf{X}_{k\text{-}1}^{\beta}$, $\mathbf{X}_{k\text{-}1}^{\delta}$ – vectors of positions of the α, β and δ wolves, respectively,
k – number of iteration of optimization algorithm,
x_i, $\boldsymbol{v}_i$ – vectors of velocity and positions the i-th particle for the PSO algorithm,
x_B – vector of leader position,
x_L – vector of best self position in previous iterations,
w_1 – weight of inertia,
c_1, c_2 – learning factors,
F^i, A^i, r^j – frequency, loudness and pulse emission of i-th bat,
ζ, γ – bat algorithm constants,
P_N, V_N, I_N, n_N, T_N – rated power, voltage, current, velocity and torque,
cosφ, η – power factor and efficiency,
$T_{\max}$ – peak torque,
l_m, g_m – length and thickness of the permanent magnet,
r_m – distance between poles,
T_{80} – electromagnetic torque for a speed of about 0,8 of synchronous speed,
B_r, H_c – residual induction and coercive force of the permanent mag net,
D_o, D_i – outer and inner diameter of the stator,
L_s – stack length,
N_s, N_r – number of the stator and the rotor slots,
d_o, d_i – outer diameter of the rotor and diameter of the shaft,
q_1, q_2, q_3 – weighting coefficient of the objective function,
$\mathbf{s}$ – the vector made up of design parameters,
$f(\mathbf{s})$, $h(\mathbf{s})$ – objective and modified objective functions,
$g(\mathbf{s})$: – non-linear constraint function,
$p(\mathbf{s})$ – penalty term,
n – number of external penalty function iteration,
σ – penalty factor,
$m_{pm}(\mathbf{s})$, m_{pm}^i – permanent magnet mass and imposed mass of the permanent magnet,
N – number of individuals in optimization procedure,
N_{of} – number of calls function.

E-mail addresses: lukasz.knypinski@put.poznan.pl

1. Introduction

At present, complex models of the various phenomena in the designed device are used in the design process. These models consist of: (a) an equation describing of the electromagnetic field, (b) supply circuit equations, (c) an equation describing rotational equilibrium and also (d) an equation describing the thermal phenomena [2, 3, 9, 11, 33]. All of these phenomena are usually taken into account when the finite element method (FEM) is used. FEM models are very complex, therefore, the optimization processes which incorporate them are very time-consuming.

Constrained optimization (CO) is the most important tool in the process of modern design of electromagnetic devices, such as: electric motors, transformers and electromagnetic actuators. The design problem must often necessarily to take into account constraints related to the dimensions of the devices and the imposed functional parameters. Solutions of these constrained problems require new, more and more effective methods of optimization.

In the optimization process the objective functions have usually economic features and are closely connected with the minimization of the production costs and power losses [19, 31]. They may also include components related to the protection of natural environment.

In international literature, intensive development of new optimization algorithms has been observed. Currently heuristic (non-deterministic) algorithms [1, 6] are being most dynamically developed. These types of optimization algorithms are especially effective in solving the design challenge connected with electromagnetic converters [8, 10]. Classification of the optimization algorithms proposed by the author is presented in Figure 1.

In the last two decades, an increased number of papers devoted to the application of different probabilistic algorithms elaborated on the basis of the natural environment (nature-inspired algorithm [36]) has been observed in relation to the design of PM motors. Among PM motors, brushless direct-current motors (BLDC) and permanent magnet synchronous motors (PMSM) are currently developing most dynamically. The Genetic Algorithm (GA) and Particle Swarm Optimization (PSO) algorithms are often used to optimize these two types of motors [7, 11, 14] and other technical problem [32]. In order to achieve a better convergence of optimization processes, scientists are continuously applying new optimization algorithms. New optimization algorithms are being used more and more often. This group of algorithms consists of: the Ant Colony Optimization (ACO) algorithm [26], the Cuckoo Search (CS) algorithm [5, 37], the Bat Algorithm (BA) [4] and the Gray Wolf Optimizer (GWO) algorithm [14]. Optimization calculations are often performed on simplified models (analytical or lumped parameters) of the PM motors [14, 26, 27]. There are not many articles on the subject of optimization algorithms using 2D FEA models and gray wolf optimization.

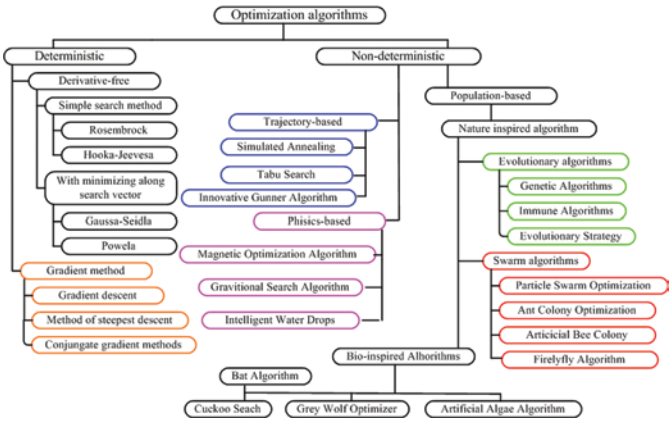

Fig. 1. The classification schema of the optimization algorithms

The aim of this paper is to develop a constrained optimization procedure based on the GWO algorithm. The developed algorithm was employed for the constrained optimization of a line-start permanent magnet motor (LSPMSM). Additionally, the convergence of the developed procedure in comparison to other nature-inspired algorithms was investigated.

The organization and social rules in a wolf-pack and the mathematical rules of the gray wolf method are presented in details and are described in section 2. Also, the main equations for the PSO and the BA are presented in section 2. Next, the algorithm and computer software for the constrained optimization of the LSPMSM are presented in section 3. In section 4, a comparison of the performance of the GWO, the PSO, the BA and the GA has been performed. The summarizing conclusions are discussed in section 5.

2. Nature inspired optimization algorithms

In general, the PSO and GA algorithms are most often used for those problems related to electromagnetic design optimization. Recently, a rapid development of metaheuristic algorithms has been observed, including: CS, BA, GWO and others. These algorithms are increasingly used to optimize and design technical devices. In the international literature, there are no papers which confirm the advantages of these algorithms over PSO and GA.

2.1. Mathematical description of the organization and social rungs in wolf pack

Wolves represent the Carnivora order and are members of the Canidae family. Wolves are social animals organized in groups called packs. Wolf demonstrates an expanded system of social rungs (hierarchy), which decide the position of each member within the wolf pack.

Each pack occupies a specific area where it lives and hunts and which it protects from other wolves. Just like any other social group, the pack needs a leader – an individual to keep the order in the group. The leader of pack is the ***alpha individual*** (α). The alpha (the most well adapted individual) always leads the wandering group, initiates attacks on other wolves infringing on the pack's territory, initiates hunting as well as all other activities of the wolf pack [20]. The wolf pack hierarchy is linear, the group leader is the wolf who won direct confrontations with other pack members. Family relations can also determine the pack's hierarchy [24]. A very important role in the pack is the ***beta wolf*** (β). This individual submits only to the alpha, while being stronger than other members of the group. For groups living in the wild, the beta individual is usually the strongest individual, but less ingenious and less intelligent than the alpha. The alpha and beta individuals are a complementary pair. The beta male is strong, brave and confident but submits to the alpha male. The beta assumes the pack leadership when the alpha leaves the group grows old or dies.

The third level of the pack hierarchy are the **δ *individuals***, which are weaker than α and β individuals but stronger than ***omega individuals*** (ω). The omega individuals form the lowest rung of the pack hierarchy [22]. They submit to all other members of the pack; they are the last to be allowed to feed and are often used as "scapegoats". Most often, the omega individuals are the oldest or frailest.

The mathematical model of the GWO algorithm was based on the wolves hunting behavior. Depending on the size of their prey, wolves can use different hunting tactics.

The wolves recognize the herds of potential victims before starting the hunt. This is the **searching for prey stage** [25]. At the beginning, the wolves choose their victim. Then the predator get very close to it. If the prey does not get scared by the predator or even starts to approach it, the wolf retreats. If the animal starts to run away, the wolves immediately start the chase. This is the **chase stage.** During the chase, the wolves often change which of them, pursues the prey. The main purpose of this tactic is to disorientate the victim. The wolves may also force the animal to change its direction of escape. After stopping the prey, wolfs immediately attack prey.

In the numerical implementation of the GWO algorithm it was assumed that the global extreme point is situated between the three leaders (α, β and δ). Thus, the vector of position for each *i*-th individual in *k*-th iteration (*k*-th time step) is determined as [17]:

$$\mathbf{X}_k^i = \mathbf{X}_{k-1}^p - A_k \left| C_k \mathbf{X}_{k-1}^p - \mathbf{X}_{k-1}^i \right|, \tag{1}$$

where A_k and C_k are the factors of the gray wolf algorithm, $\mathbf{X}_{k-1}^p$ is the location vector of the prey (the global extreme).

The factor A_k and C_k are different for the α, β and δ individuals in the developed algorithm and are calculated as follows:

$$A_k^\alpha = 2b_k r_1 \quad A_k^\beta = 2b_k r_2 \quad A_k^\delta = 2b_k r_3, \tag{2}$$

$$C_k^\alpha = 2r_4 \quad C_k^\beta = 2r_5 \quad C_k^\delta = 2r_6, \tag{3}$$

in which: r_1 to r_6 are the numbers randomly selected from range (0, 1), b_k is the factors which describes the ability of wolves to migrate in the permissible area of the solved task. In the case of a large value of this parameter the individuals can move freely in the area of the considered task. The algorithm then has the properties of a global search algorithm. A low value of this parameter means the algorithm has the properties of a local search method. The value of the *b* parameter is usually decreased from 2 to 0 [17, 25].

In the developed algorithm the author proposed a decrease in the value of the coefficient during the process of optimization. The value of *b* in subsequent *k*-th iterations is calculated according to the following formula [15]:

$$b_k = 0.97 + 5e^{-k}. \tag{4}$$

According to the developed procedure the three best-adapted wolves are represented as individuals α, β and δ. Thus, there is one α, one β and one δ in each iteration. In order to determine the new position of *i*-th ω individual, it is necessary to calculate the distance of this individual from the best wolves in the pack [38]:

$$D^\alpha = \left| C_k^\alpha \mathbf{X}_{k-1}^\alpha - \mathbf{X}_{k-1}^i \right|, \quad D^\beta = \left| C_k^\beta \mathbf{X}_{k-1}^\beta - \mathbf{X}_{k-1}^i \right|, \quad D^\delta = \left| C_k^\delta \mathbf{X}_{k-1}^\delta - \mathbf{X}_{k-1}^i \right|, \tag{5}$$

where: $\mathbf{X}_{k-1}^\alpha$, $\mathbf{X}_{k-1}^\beta$ and $\mathbf{X}_{k-1}^\delta$ denote the positions of the three best individuals (α, β and δ) in the previous iteration.

Finally, the new position for each *i*-th ω individual in the *k*-th iteration (*k*-th time step) is determined using the following equation:

$$(\mathbf{X}^\omega)_k^i = \frac{\mathbf{X}_1^\alpha + \mathbf{X}_2^\beta + \mathbf{X}_3^\delta}{3}, \tag{6}$$

where: $\mathbf{X}_1^\alpha = \mathbf{X}_{k-1}^\alpha - A_k^\alpha D^\alpha$, $\mathbf{X}_2^\beta = \mathbf{X}_{k-1}^\beta - A_k^\beta D^\beta$, $\mathbf{X}_3^\delta = \mathbf{X}_{k-1}^\delta - A_k^\delta D^\delta$.

The flowchart of the GWO method is illustrated in Figure 2.

2.2. The classical Particle Swarm Optimization

The classical PSO algorithm was developed in 1995 [30]. This algorithm mimics the foraging behavior of flocks of birds and fish shoals. The optimization process uses the interaction between the leader (the best particle in the group) and the rest of the particles. All of the particles form the swarm system. The best-adapted particle is

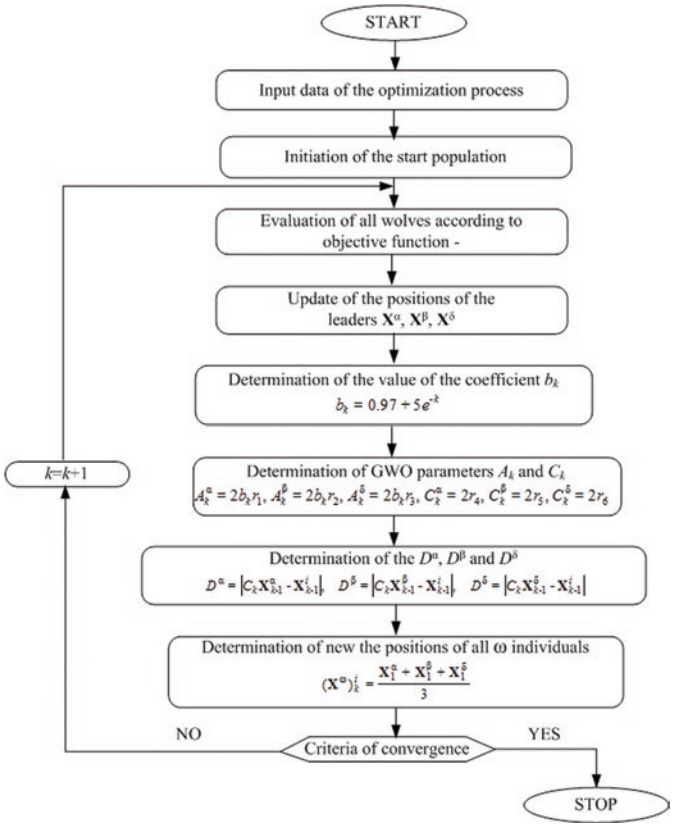

Fig. 2. The block diagram of the elaborated GWO algorithm

the leader of the swarm. Each particle is described by two vectors: (a) the position vector ($\mathbf{x}^i$) and (b) the velocity vector ($\mathbf{v}^i$). In order to determine the new position of the *i*-th particle, the position vector of the leader ($\mathbf{x}_B$), the local best known position of the *i*-th particle and the vector of velocity from the previous iteration are taken into account. The velocity vector of the *i*-th particle in the *k*-th iteration is calculated according to the following formula:

$$\mathbf{v}_k^i = w_1 \mathbf{v}_{k-1}^i + c_1 r_1 \left(\mathbf{x}_L^i - \mathbf{x}_{k-1}^i \right) + c_2 r_2 \left(\mathbf{x}_B - \mathbf{x}_{k-1}^i \right), \tag{7}$$

where: w_1 is the weight of inertia, c_1 and c_2 are the learning factors, r_1, r_2 are the random numbers from range (0, 1), $\mathbf{x}_B$ is the position vector of the swarm leader and $\mathbf{x}_L$ is the vector of the best location of the *i*-th particle in the previous iteration.

Finally, the position of the *i*-th particle is determined as follows:

$$\mathbf{x}_k^i = \mathbf{x}_{k-1}^i + \mathbf{v}_k^i. \tag{8}$$

2.3. The Bat Algorithm

The Bat Algorithm (BA) was developed in 2010 [34]. The mathematical model of the BA is based on the echolocation navigation of small species of bats. Each bat is characterized by a velocity vector ($\mathbf{v}^i$), a position vector ($\mathbf{x}^i$), varying frequency (F^i), loudness (A^i) and pulse emission (r^i). A group of bats constitutes a bat colony. The search of the global extreme is carried out by randomly searching the permissible area. The individual with the best objective function value is the colony leader. The position of the leader is updated in every *k*-th iteration of the algorithm. The position vector of *i*-th bat is calculated using: the position of the best bat in the colony, the velocity vector of *i*-th bat from the previous iteration and the random value of frequency. The position of each bat is determined as follows:

$$\mathbf{x}_k^i = \mathbf{x}_{k-1}^i + \left[\mathbf{v}_{k-1}^i + F^i \left(\mathbf{x}_{k-1}^i - \mathbf{x}_B \right) \right], \tag{9}$$

$$F^i = F_{\max} + r(F_{\max} - F_{\min}) , \quad (10)$$

where: r is a randomly selected number from the range (0, 1); $F_{\max}$ and $F_{\min}$ are the maximum and minimum frequency values.

In each step of the algorithm, a test modification of the leader/random individual is performed, this represents the local search capability. The test position **x*** near the leader/random bat is determined as follows:

$$(\mathbf{x}^*)_k^i = \mathbf{x}_k^i + \kappa A_{av} \quad (12)$$

where: κ is a randomly selected number from the range (0, 1), A_{av} is the value of the average loudness of a bat colony in the j-th time step.

If the test position $(\mathbf{x}^*)_k^i$ has a better objective function value than $\mathbf{x}_k^i$, then $\mathbf{x}_k^i$ is updated by **x***. The loudness A^i and rate of pulse emission r^i of a bat in the next iteration are calculated as follows:

$$A_{k+1}^i = \zeta A_k^i , \; r_{k+1}^i = r_0[1-\exp(-\gamma j)] \quad (13)$$

in which: ζ and γ are the bat algorithm constants, r_0 is the initial value of emission rate.

3. Constrained optimization of PM synchronous motor

The GWO algorithm is very often applied for the purpose of solving global optimization problem. However, there are not too many articles in international literature regarding the application of this method to solve constrained optimization tasks [13, 17]. Moreover, in the case of optimization of PM motors the simplified model of phenomena is usually applied.

In order to validate the effectiveness and performance of the GWO algorithm in combination with the external penalty function, constrained optimization of the LSPMSM has been performed. The in-house optimization software consists of two independent modules: (a) the optimization module and (b) the numerical model of PM motor. The optimization module comprises the gray wolf algorithm and was developed using Delphi 7.0. The non-linear constraint was taken into account through the external penalty function [35]. The numerical model of the LSPMSM was developed in the ANSYS Maxwell environment using 2D finite element method (FEM). This model consist two independent 2-D FEM transient models: (a) a steady-state operation model at synchronous speed and (b) a model describing start-up of motor. The efficiency and power factor under the rated load condition was calculated in the steady-state operation model. The model which describes the start-up allows for the calculation of the value of electromagnetic torque during the start-up of the motor. A stator from a serially manufactured six-poles induction motor, type MS2 132M-6 was applied. The rated parameters of the MS2 132M-6 motor are listed in Table 1.

Table 1. Rated parameters of the MS2 132M-6 type motor

Parameter	Symbol	Value	Unit
Rated output	P_N	5,5	kW
Rated voltage	V_N	400	V
Rated current	I_N	12	A
Rated speed	n_N	960	rpm
Efficiency	η	86	%
Power factor	cosφ	0,78	-
Rated torque	T_N	54,7	Nm
Peak torque	T_{max}	147,1	Nm

The stator winding has a three-phase, a double-layer which overlaps the whole-coiled winding. The winding is wye-connected. The main dimensions of the stator and the rotor of the induction motor are listed in Table 2.

Table 2. Main stator and rotor dimensions of the MS2 132M-6 type motor

Parameter	Symbol	Value	Unit
Outer stator diameter	D_o	240	mm
Inner stator diameter	D_i	165	mm
Length of stator core	L_s	115	mm
Number of slot in stator	N_s	54	–
Outer rotor diameter	d_o	164,2	mm
Shaft diameter	d_i	45	mm
Number of slots in rotor	N_r	51	–

The optimization task consists of such a selection of the structure of the rotor, which include cage winding made of aluminium and permanent magnets. Only the dimension of the permanent magnet and its location in the rotor structure were taken into account. Three design parameters were adopted: $s_1 = l_m$ – magnet length, $s_2 = g_m$ – magnet thickness and $s_3 = r_m$ – distance between poles (see Figure 3). The ranges of the design variables are presented in Table 3. During study, the all stator dimensions and winding parameters represented constants.

Table 3. The range of the design variables

Variable	Structure parameter	Down	Up
s_1	l_m	1 mm	16 mm
s_2	g_m	2 mm	12 mm
s_2	r_m	5 mm	67 mm

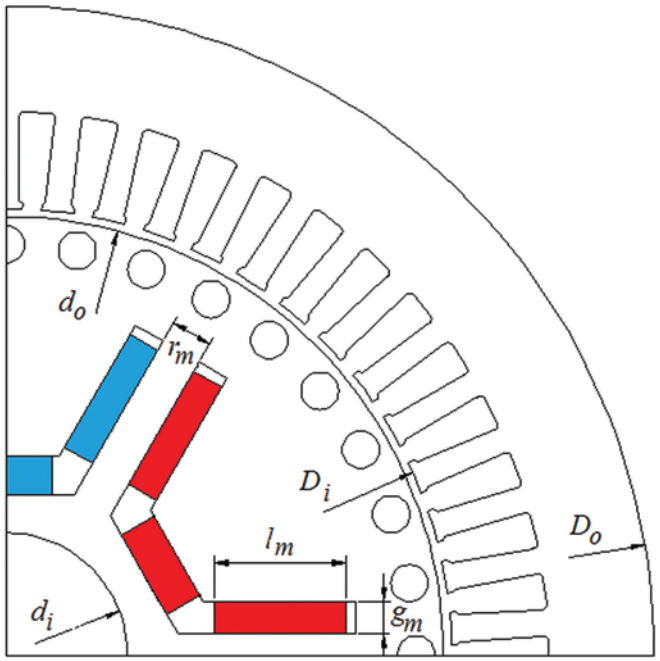

Fig. 3. The structure of discussed LSPMSM

The air gap in the designed LSPMSM motor was increased to 0,8 mm in comparison to the MS2 132M-6 induction motor. The air gap

extension was obtained by reducing the outer diameter of the rotor d_o. The permanent material NdFeB N33 with nominal magnetic properties: B_r = 1,15 T and H_c = 836 kA/m was applied.

An optimal motor should be characterized by high values of three maintenance (functional) parameters: (a) efficiency [18], (b) power factor and (c) synchronization capability. The synchronization capability is determined by value of the electromagnetic torque for a speed equal 0,8 of the synchronous speed. In the case of induction motors, a speed of about 0,8 of synchronous speed is the highest value of electromagnetic torque, i.e. the peak torque. During the LSPMSM start–up process we can observe two types of torque [39]. The first one is the asynchronous torque generated by squirrel cage winding, where slips differ from 0. The second one is the synchronous torque, which includes (a) the opposite braking torque generated by the permanent magnet and (b) the reluctance torque [23]. The braking torque depends on the dimensions of the permanent magnets. The reluctance torque is generated by the diversity of the rotor structure in which gaps for permanent magnets are present. The braking torque degrades the line-start performance. The total electromagnetic torque generated by a machine during the synchronization period is the sum of the synchronous and the asynchronous torques. Figure 4 illustrates the waveform of the total torque, the sum of the asynchronous and the reluctance torque and the opposite torque generated by the PM during the start-up of the LSPMSM. The presented torque-slip curves were calculated for a machine obtained in the start population. It can be observed, that magnets with excessively large dimensions were used in the studied LSPMSM. The motor was characterized by a high value of opposite torque generated by the PM. The high value of the opposite torque significantly weakens the value of the asynchronous torque. As a result of this, the motor can have problems when going into the synchronous state. The authors of papers concerning the optimization of the LSPMSM very frequently use the T_{80} value to guarantee a proper synchronization process [11, 12].

In the case of multi-criteria optimization problems, two types of compromise objective functions can be applied: (a) multiplicative and (b) additive [28]. After performing many computational simulations for the three iterations of the GWO algorithm, it was observed that the multiplicative function is more sensitive to changes in functional parameters than the additive function. During the optimization of the LSPMSM the most important parameter is the synchronization capability; in the case of multiplicative function the obtained values of this parameter were better. Thus, in the developed algorithm, the objective function for j-th wolf has been defined as follows:

$$f^j(\mathbf{s}) = \left(\frac{\eta^j(\mathbf{s})}{\eta_0}\right)^{q_1}\left(\frac{\cos\varphi^j(\mathbf{s})}{\cos\varphi_0}\right)^{q_2}\left(\frac{T_{80}^j(\mathbf{s})}{T_0}\right)^{q_3}, \tag{13}$$

where s=[s_1, s_2, s_3]^T is the vector made up of design parameters, $\cos\varphi^j(\mathbf{s})$, $\eta^j(\mathbf{s})$ and $T_{80}^j(\mathbf{s})$ represent the power factor, the efficiency and the out put torque at a speed equal to 0,8 of the synchronous speed, η_0, $\cos\varphi_0$ and T_0 are the values of these 3 parameters calculated as a mean value of such parameters from 15 runs of optimization procedure for random distribution of the start wolf pack before the start of the optimization process, q^1, q^2 and q^3 are the weighting coefficients.

Moreover, an economic factor has been taken into account during the optimization process and the consumption of the permanent magnet material was included into the design process. The non-linear constraint concerning the total mass of permanent magnet material was defined as $m_{pm}^j(\mathbf{s}) \le m_{pm}^i$, where m_{pm}^i is the imposed total mass of permanent magnet material in the designed motor. The non-linear constraint function has been normalized and calculated as:

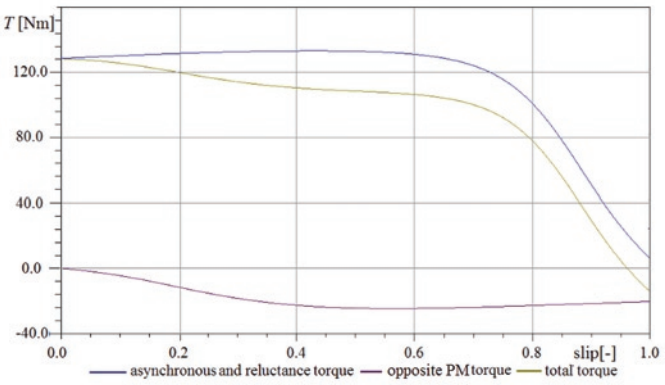

Fig. 4. The torque components during start-up process of LSPMSM

$$g^j(\mathbf{s}) = \frac{m_{pm}^j(\mathbf{s}) - m_{pm}^i}{m_{pm}^i}. \tag{14}$$

The imposed constraint was included in the optimization process by using the external penalty function [35]. In the penalty function approach, the modified objective function $h(\mathbf{s})$ is created. The $h(\mathbf{s})$ function is composed of: (a) objective function $f(\mathbf{s})$ and (b) penalty term $p(\mathbf{s})$. The penalty term $p(\mathbf{s})$ for the j-th wolf is calculated as follows:

$$p^j(\mathbf{s}) = \sigma^n g^j(\mathbf{s}). \tag{15}$$

In the developed algorithm, the iterations related to a change in external penalty (n) are intertwined with iterations of the GWO algorithm (k). The value of the penalty coefficient is modified after performing three iterations of the GWO algorithm. In each subsequent iteration of the penalty (n), the penalty coefficient value is increased. After performing the maximum number of penalty iterations (n_{max}), the optimization process is finished.

In the developed algorithm the objective function $f(\mathbf{s})$ is maximized. Therefore, the modified objective function $h(\mathbf{s})$ is defined as follows:

$$h^j(\mathbf{s}) = \begin{cases} f^j(\mathbf{s}) & \text{for} \quad m_{pm}(\mathbf{s}) \le m_{pm}^i \\ f^j(\mathbf{s}) - p^j(\mathbf{s}) & \text{for} \quad m_{pi}(\mathbf{s}) > m_{pm}^i \end{cases}. \tag{16}$$

4. Simulation results for different optimization algorithms

In order to evaluate the convergence and reliability of the developed optimization procedure (containing the gray wolf algorithm), test calculations which consisted of the constrained optimization of a LSPMSM motor were performed. All the studied optimization procedures were developed by the author in the Borland Delphi 7.0 environment. The optimization procedures containing each method (GWO, PSO, BA and GA) were repeated 12 times. The best results obtained from all runs of the optimization software for the GWO algorithm were compared with those of the PSO, the BA and the GA in Tables 4, 5, 6, 7 and 8. Next, statistical analysis of the results was performed for all of the optimization algorithms used.

4.1. Calculations for the GWO method

The optimization calculation was performed for a wolf pack size equal to 32 individuals. Due to the application of the FEM model of the LSPMSM, such a number of individuals provided a compromise between good convergence of the optimization procedure and the calculation time. The following parameters of the optimization proce-

Table 4. The course of the constrained optimization of LSPMSM for α wolf

k	r_m	g_m	l_m	$\eta(s)$	$cos\varphi(s)$	$T_{80}(s)$	$m_{pm}(s)$	$h(s)$	N_{of}
	mm	mm	mm	%	-	Nm	kg	-	-
1	7,16	6,85	43,38	91,01	0,808	96,845	1,518	2,786569	61
2	6,98	3,28	56,57	90,86	0,807	120,661	0,948	3,358127	88
3	8,09	4,90	64,42	91,81	0,940	102,498	1,612	3,370711	119
5	6,97	4,61	65,10	91,76	0,933	105,709	1,529	3,488402	177
7	6,05	4,45	64,98	91,73	0,927	106,567	1,477	3,505084	235
9	8,08	4,54	64,89	91,76	0,931	106,115	1,508	3,507330	293
10	8,49	4,53	64,81	91,76	0,931	106,163	1,503	3,508139	322
12	9,58	4,50	64,79	91,75	0,930	106,219	1,498	3,509258	380
15	9,49	4,49	64,79	91,75	0,930	106,500	1,499	3,516157	467
20	9,49	4,49	64,79	91,75	0,930	106,500	1,499	3,516157	612
30	9,49	4,49	64,79	91,75	0,930	106,500	1,499	3,516157	902

Table 5. The course of the constrained optimization of LSPMSM for β wolf

k	r_m	g_m	l_m	$\eta(s)$	$cos\varphi(s)$	$T_{80}(s)$	$m_{pm}(s)$	$h(s)$
	mm	mm	mm	%	-	Nm	kg	-
1	9,18	6,32	36,08	90,214	0,739	107,329	1,165	2,767361
2	11,38	5,36	52,66	91,405	0,860	103,287	1,442	3,158777
3	11,98	4,84	54,38	91,382	0,860	107,259	1,344	3,257946
5	7,86	4,82	64,62	91,812	0,941	103,193	1,598	3,403105
7	11,29	4,52	65,03	91,764	0,932	105,577	1,500	3,497235
9	9,58	4,50	64,97	91,752	0,930	106,219	1,495	3,502258
10	10,13	4,51	65,84	91,759	0,931	105,960	1,498	3,504899
13	8,01	4,53	64,97	91,757	0,931	106,246	1,503	3,509144
15	9,63	4,52	64,92	91,758	0,931	106,138	1,499	3,509673
30	9,37	4,50	64,81	91,753	0,930	106,327	1,499	3,511512

dure were assumed: q_1=1, q_2=4/5, q_3=1/3, m_{pm}^i =1,5 kg and σ=1,2. The penalty coefficient was increased in every third internal iterations of the GWO method. As a stop criteria, a maximum number of external iterations n_{max}=10 was assumed, i.e. 30 iterations of the GWO method. The following values of reference parameters were adopted: η_0=81,325 %, $\cos\varphi_0$=0,753 and T_0=50,124 Nm. Such values was the same for all investigated optimization procedures.

The results of the optimization calculation for the selected GWO iterations are presented in Tables 4 and 5. The results for the α individual are reported in Table 4, while the results for the β individuals are listed in Table 5. In the successive columns, the design parameters values (r_m, g_m, l_m), the functional parameters (η, cosφ and T_{80}) of the designed motor, the modified objective function value (h), and the number of calls function (N_{of}), i.e. number of calculations of the objective function are listed.

The calculations were made on a computer with the following parameters: processor: Ryzen 5 six-core, 3,40 GHz and 16,0 GB RAM. The calculation time for one individual is equal to 8 minutes and 6 seconds. The calculation time depends on the saturation, especially at the initiation of the wolf pack. The approximate calculation time for the optimization process was about 116 hours for a single computer. The developed optimization procedure was tested and a good convergence was achieved. It should be noted that the developed algorithm determined the optimal solution after about 12 iterations, i.e. after four iterations related to the increasing penalty, and the imposed total mass of permanent material was attained. In the successive iteration of optimization process, the maximized functional parameters were improved.

4.2. Calculations for the PSO algorithm

Next, the calculations for the classical PSO algorithm were performed. The number of particles was N=32. The following values of the PSO coefficients were assumed: w=0,2, c_1=0,35 and c_2=0,45. The values of the PSO coefficients were assumed on the basis of many computer simulations to provide good convergence of the optimization procedure for the first three iterations. The PSO algorithm was combined with an external penalty. The parameters of the optimization procedure are the same as the parameters of the GWO algorithm. The course of the optimization process for the selected iterations is presented in Table 6.

The total approximate calculation time in case of PSO optimization procedure is 132 hours. The computation time for the PSO method is slightly longer than for the GWO method. Moreover, the obtained result is lower quality in comparison to the GWO algorithm.

4.3. Calculations for the BA algorithm

Thus, the constrained optimization process was executed for the BA algorithm. The number of bats in a colony was N=32 and the maximum external penalty iteration is equal to n_{max}=10. The adopted values of the BA parameters were based on the author's previous experience. The following values have were adopted: range of frequency F_{min}=0, F_{max}=1,0, initial pulse emission value r_0=0, and initial

Table 6. The course of the constrained optimization of LSPMSM for PSO algorithm

k	r_m	g_m	l_m	$\eta(s)$	$cos\varphi(s)$	$T_{80}(s)$	$m_{pm}(s)$	$h(s)$	N_{of}
	mm	mm	mm	%	-	Nm	kg	-	-
1	9,68	8,20	40,69	90,081	0,692	107,672	1,7042	2,594397	64
2	9,68	7,07	42,21	90,950	0,801	95,928	1,5242	2,750185	96
3	10,86	6,93	61,41	92,007	0,990	74,609	2,3010	2,806432	128
5	8,33	4,56	63,87	91,764	0,932	105,855	1,5142	3,507002	192
10	9,16	4,52	64,08	91,757	0,931	106,151	1,4991	3,509267	352
13	9,16	4,52	64,08	91,757	0,931	106,151	1,4991	3,509267	448
14	8,90	4,52	64,65	91,757	0,931	106,176	1,5001	3,510162	480
20	9,04	4,52	64,65	91,756	0,930	106,193	1,4996	3,510163	672
23	9,35	4,50	64,66	91,754	0,930	106,283	1,4994	3,510606	768
25	9,44	4,51	64,72	91,755	0,930	106,255	1,4998	3,510748	832
30	9,50	4,49	64,82	91,752	0,930	106,333	1,4998	3,510911	992

Table 7. The course of the constrained optimization of LSPMSM for BA algorithm

k	r_m	g_m	l_m	$\eta(s)$	$cos\varphi(s)$	$T_{80}(s)$	$m_{pm}(s)$	$h(s)$	N_{of}
	mm	mm	mm	%	-	Nm	kg	-	-
1	7,79	8,90	47,53	91,824	0,906	71,773	2,160	2,218321	64
3	9,78	8,27	41,15	90,141	0,697	105,722	1,738	2,573938	128
5	9,78	8,27	41,15	90,141	0,697	105,722	1,738	2,573938	192
7	6,20	6,79	53,69	91,685	0,899	89,486	1,861	2,942079	256
10	6,20	6,79	53,69	91,685	0,899	89,486	1,861	2,942079	352
14	4,97	5,68	62,06	91,861	0,945	95,951	1,801	3,281955	480
18	9,43	4,47	60,65	91,588	0,896	108,529	1,385	3,439104	576
20	7,68	4,59	62,71	91,692	0,916	106,836	1,468	3,471697	672
22	6,34	4,50	64,13	91,746	0,929	106,929	1,495	3,506710	736
24	3,49	4,50	64,52	91,737	0928	107,548	1,495	3,514491	800
28	3,31	4,52	64,78	91,741	0,928	107,425	1,500	3,516855	928
30	3,45	4,52	64,78	91,741	0,929	107,386	1,500	3,517128	992

loudness value A_0=1, ζ=0,7 and γ=0,6. The results of the optimization process for the selected time steps are presented in Table 7. In the successive columns, the number of time steps, the coordinates of the best bat (individual), the modified objective function for the leader of a bat colony and the number of call function are listed.

In the case of the BA algorithm, the obtained approximate operating time of the optimization procedure is similar to the PSO and equal 132 hours.

4.4. Calculations for the GA algorithm

Also, the calculations for GA procedure for parameters: population size equal N=32, probability of mutation p_m=0,007 were executed. The optimization procedure consists of three genetic operators: reproduction, crossover and mutation [27]. Additionally, the simple elitism procedure has been applied to save the best individual during genetic operations, especially mutation procedure. The roulette wheel reproduction and one cut-point in chromosome crossover methods have been applied. Also, improved crossover procedure was applied. The crossover procedure consists of two phases. First, all individuals are crossover. The new generation was created from the best half of parents and the best half of children [16]. Such a crossover operation significantly improves the convergence of an elaborated optimization procedure based on genetic algorithm. The GA optimization procedure is adapted to perform optimization calculation by the use of the FEM models. In each genetic generation, the values of objective function are calculated only for new individuals created in crossover and mutation procedures. The course of the optimization process for the selected genetic iterations is presented in Table 8.

The total calculation time for GA was the longest from all the tested algorithms and was equal 195 h. However, the obtained result was the best.

4.5. Statistical analysis of all the tested methods

On the basis of the obtained results it can be noted, that the investigated optimization algorithms (GWO, PSO, BA and GA) correctly found the global maximum. Similar values of design variables were determined for the GWO and the PSO algorithms. After about 12 iterations, i.e. 380 calls of objective function, the gray wolf algorithm determined a solution which was close to optimal. The value of the modified objective function for the α individual improved in subsequent iterations (see Table 4). In comparison with the PSO algorithm, the β individual has much more accurate results than the PSO leader. The PSO method provided the least accurate solution from among all the tested methods. It can be observed that for the PSO algorithm, the modified objective function value was improved until the last iteration of the algorithm. The highest value of the objective function was obtained for GA.

The convergence process for all the studied algorithms is presented in Figure 5. The fastest convergence at the beginning of the optimiza-

Table 8. The course of the constrained optimization of LSPMSM for GA

k	r_m	g_m	l_m	$\eta(s)$	$cos\varphi(s)$	$T_{80}(s)$	$m_{pm}(s)$	$h(s)$	N_{of}
	mm	Mm	mm	%	-	Nm	kg	-	-
1	11,99	8,68	40,53	91,283	0,830	75,827	1,795	2,353208	127
2	11,97	7,44	65,00	92,022	0,981	58,508	2,469	2,365551	173
3	6,87	5,12	58,24	91,629	0,899	103,787	1,524	3,321283	217
5	4,98	4,18	57,03	91,299	0,854	113,598	1,217	3,392834	296
7	3,71	4,49	63,38	91,681	0,916	108,336	1,454	3,509650	384
9	9,03	4,52	65,00	91,756	0,931	106,181	1,499	3,509902	501
11	8,07	4,52	64,88	91,754	0,930	106,395	1,500	3,514408	568
13	7,59	4,52	64,88	91,752	0,930	106,512	1,499	3,516853	659
16	7,69	4,51	64,92	91,750	0,930	106,600	1,499	3,517968	792
20	7,25	4,52	64,87	91,751	0,930	106,605	1,499	3,518801	973
30	7,25	4,52	64,88	91,751	0,930	106,605	1,499	3,518801	1463

tion process was provided by the GWO algorithm. The BA algorithm was characterized by the worst convergence.

The process of searching for the global maximum in the case of the BA algorithm is very interesting. On the basis of the data presented in Figure 5, it can be observed that every few iterations, there is a change in the position of the best adapted bat. In the BA method the individuals move randomly around the best bat. The result, which is close to the optimal one is obtained after 24 time steps of the BA algorithms, i.e. after 800 calls of the objective function. This is double the number of the calls function than in the case of the GWO.

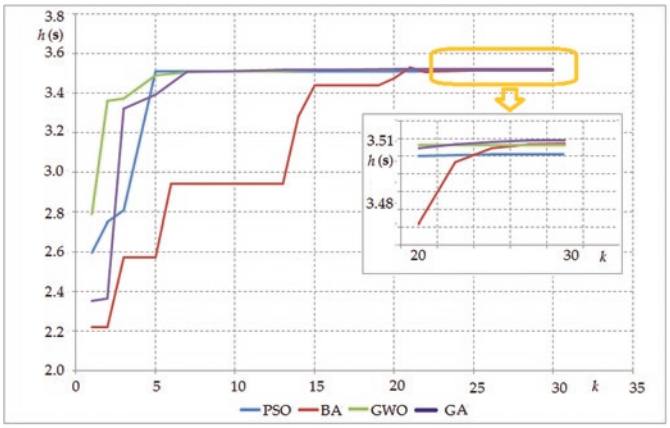

Fig. 5. Convergence curves for investigated methods

Subsequently, the changes of the design variables during the optimization process were analyzed. Figure 6 shows the variation of all design variables in successive iterations of the optimization process.

It can be observed, that in the case of the distance between the poles (r_m), the design variables changed during the optimization process. As a result of the optimization process for the PSO and the GWO algorithms, similar "optimal" values were received (see Figure 6a). However, for the BA and GA a different "optimal" value of the (r_m) variable than for the other tested algorithms were obtained. In the case of the magnet length (l_m), as a result of the optimization process, a similar PM magnet length value was obtained for all the examined optimization algorithms (see Figure 6). It was also observed, that the BA convergence was the worst when compared with the other algorithms. For the magnet thickness (g_m) for all the optimization algorithms, similar of the optimal value of this design parameter were obtained.

The results were obtained during 12 runs of the optimization software for different optimization procedures. For all the optimization algorithms, the best, and the worst solution, as well as the average and

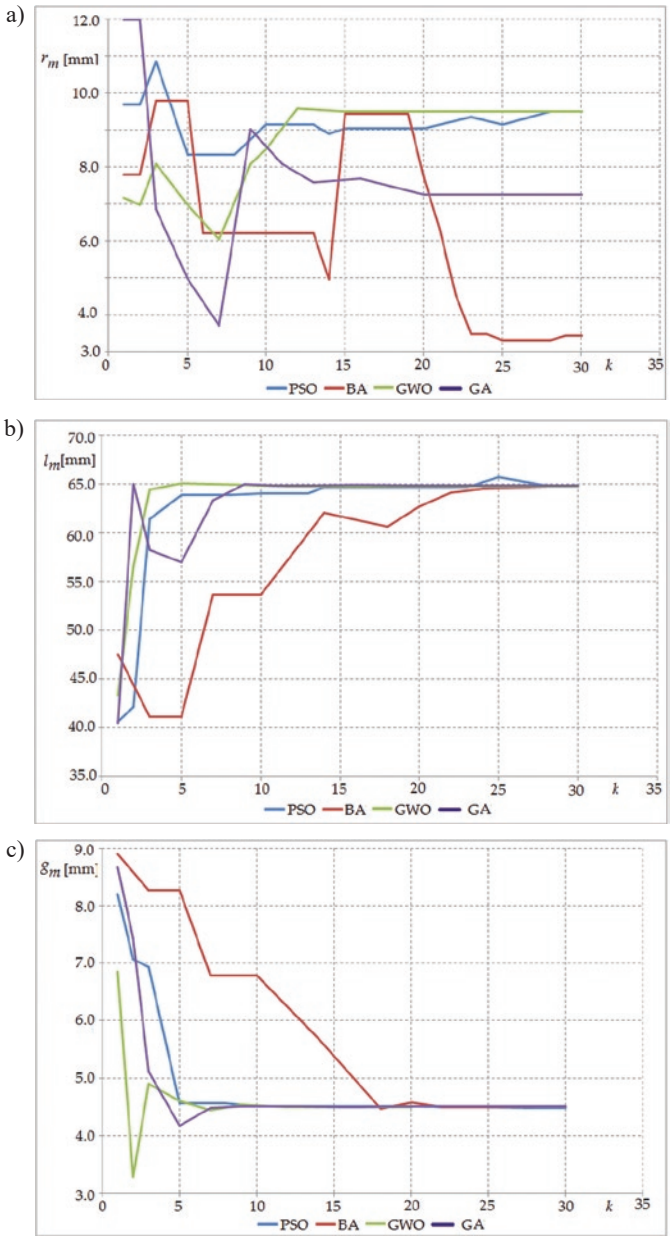

Fig. 6. Variations of design variables in successive iteration of the optimization process: (a) r_m, (b) l_m and (c) g_m.

Table 9. Statistical data for 12 runs of optimization software

Algorithm	Best	Worst	Mean	Standard deviation	Approximate calculation time
GWO	3,516157	3,490543	3,501622	0,009157	116 h
PSO	3,510914	3,456814	3,490405	0,017013	132 h
BA	3,517136	3,426121	3,488883	0,025126	132 h
GA	3,518801	3,476884	3,501936	0,015807	195 h

standard deviation were determined. The obtained results are shown in Table 9.

The best value of the objective function was obtained for the BA. However, the other best results (mean value, worst objective function value and standard deviation) were attained in the GWO algorithm. The PSO algorithm achieved the worst optimal value of the modified objective function and the worst mean value among the investigated algorithms. While, the worst value of the standard deviation for 12 runs of the optimization procedure was obtained for the BA.

5. Conclusions

In the article the optimization procedure for the constrained optimization problem was developed. The optimization procedure is a combination of the gray wolf algorithm and the external penalty function. The procedure was applied to optimization of the LSPMSM. The designed motor was described by the FEM model. The multiplicative compromise objective function composed of three parameters of the motor has been used. Additionally, the non-linear constraint function concerning the mass of the permanent magnet material was taken into consideration.

The performance reliability of the developed optimization procedure containing the GWO algorithm was compared with other nature-inspired optimization algorithms (PSO and BA). All the investigated optimization procedures were developed in Delhi 7.0 environment. In the GWO, the results close to the optimal one can be reached almost two times faster in comparison to the BA. Of course the BA enables to obtain more accurate solution. In the computational experiment, the worst value of objective function was obtained for the PSO method. Furthermore, the GWO algorithm allows obtaining the best standard deviation and average values of objective function in the constrained optimization of the LSPMSM.

A comparison of the quality of results between alpha individual and alternative leader (β individual) was presented. A much precise optimal solution was obtained for the α wolf than for the β wolf. The beta individual has a higher value of the objective function than the leader for the PSO algorithm, which underlines the advantage of the GWO algorithm over the PSO.

In the GWO algorithm, the new positions of the omega individuals in subsequent iterations are determined on the basis of the position of the leader and two alternative leaders (β and δ individuals). This feature causes high-efficiency in comparison to other investigated methods. For the majority of nature-inspired method, in order to determine the new position of individuals only the position of the leader is taken into account. Including only the leader position may lead to a movement of the swarm/colony towards the local extreme, which causes a disturbance in the optimization process. Therefore, taking into account several leaders with different rungs can improve the performance of the optimization algorithm. The presented results are very encouraging and show clearly that the GWO method is a very interesting optimization tool.

The developed optimization procedure can be successfully applied to an optimization of different electromagnetic devices described by models of varying complexity.

In the future research, the author will build a prototype of the PM motor and will perform an experimental verification.

Acknowledgements

The presented research is supported by the project under agreement number 0212/SBAD/0521.

References

1. Amoiralis E I, Tsili M A, Kladas A G. Global transformer design optimization using deterministic and non-deterministic algorithms, Proceedings of the International Conference on Electrical Machines, Marssille, France, 2-5 September 2012, https://doi.org/10.1109/ICElMach.2012.6350207.
2. Bacchus A, Tounzi A, Arguad J. P, Bouriquet B, Biet L, Macaire L, Le Menach Y. Estimation of FEM model parameters using data assimilationand its application to an electrical machine. IEEE Transactions on Magnetics 2016; 52(3), https://doi.org/10.1109/TMAG.2015.2495265.
3. Barański M, Szeląg W, Łyskawiński W. An analysis of a start-up process in LSPMSMs with aluminum and copper rotor bars considering the coupling of electromagnetic and thermal phenomena, Archives of Electrical Engineering 2019; 68(4): 933 - 946.
4. Bora T. C, Coelho L, Lebensztajn L. Bat-inspired optimization approach for brushless DC motor problem. IEEE Transactions on Magnetics 2012; 48(2): 947 - 950, https://doi.org/10.1109/TMAG.2011.2176108.
5. Cvetkovski G, Petkovska L, Leflcy P. Cuckoo search as a tool for optimal design of PM brushless DC motor. COMPEL 2018; 37(5): 1732 -1743, https://doi.org/10.1108/COMPEL-01-2018-0025
6. Deng S, Brisset S, Clenet S. Comparative study of method for optimization of electromagnetic devices with uncertainty. COMPEL 2018; 37(2): 704 - 717, https://doi.org/10.1108/COMPEL-11-2016-0502.
7. Gao J, Liu J, Huang S, Huang K. Optimum Design of Permanent Magnet Synchronous Motor Based on Gene Handling Genetic Algorithms, Proceedings of the International Conference on Electrical and Control Engineering, Wuhan, China, 25-27 June 2010, https://doi.org/10.1109/iCECE.2010.358.
8. Hossain Mohammadi M, Silva R, Lowther D. A. Finding optimal performance indices of synchronous AC motors. IEEE Transactions on Magnetics 2017; 53(6), https://doi.org/10.1109/TMAG.2017.2662705.
9. Idziak P, Kowalski K, Nowak L, Knypiński Ł. FE transient analysis of the magnetostrictive actuator. International Journal of Applied Electromagnetics and Mechanics 2016; 51 (S1): 81 - 87, https://doi.org/10.3233/JAE-2011.
10. Ilea D, Radulescu M. M, Gillon F, Brochet P. Particle-swarm optimized design of switched reluctance motors for light electric traction applications. Electromotion Journal 2010; 17(3): 23 - 29, https://doi.org/10.1109/VPPC.2010.5729005.
11. Jedryczka C, Knypiński Ł, Demenko A, Sykulski J. Methodology for cage shape optimization of a permanent magnet synchronous motor under line start condition. IEEE Transactions on Magnetics 2018; 54 (3), https://doi.org/10.1109/TMAG.2017.2764680.

12. Jedryczka C, Wojciechowski R, Demenko, A. Influence of squirrel cage geometry on the synchronization of the line start permanent magnet synchronous motor. IET Science, Measurement & Technology 2015; 9(2): 197 - 203, https://doi.org/10.1049/iet-smt.2014.0198.
13. Joshi H, Arora S. Enhanced grey wolf optimisation algorithm for constrained optimisation problems. International Journal of Swarm Intelligence 2017; 3(2/3): 126 - 152, https://doi.org/10.1504/IJSI.2017.087871.
14. Karnavas Y L, Chasiotis I D, Peponakis E L. Permanent magnet synchronous motor design using grey wolf optimizer algorithm. International Journal of Electrical and Computer Engineering 2016; 6(3): 1353 - 1362, https://doi.org/10.11591/ijece.v6i3.9771.
15. Knypiński Ł. Adaptation of the penalty function method to genetic algorithm in electromagnetic devices designing. COMPEL 2019; 38 (4): 1285-1294, https://doi.org/10.1108/COMPEL-01-2019-0010.
16. Knypiński Ł, Nowak L. The algorithm of multi-objective optimization of PM synchronous motors. Przegląd Elektrotechniczny 2019; 95 (4): 242-245, https://doi.org/10.15199/48.2019.04.46.
17. Kohli M, Arora S. Chaotic grey wolf optimization algorithm for constrained optimization problems. Journal of Computational Design and Engineering 2018; 5: 458 - 472, https://doi.org/10.1016/j.jcde.2017.02.005.
18. Kosucki A, Stawiński Ł, Malenta P, Zaczyński J, Skowrońska J. Energy consumption and energy efficiency improvements of overhead crane's mechanism. Eksploatacja i Niezawodnosc - Maintenance and Reliability 2020; 22(2): 232 - 330, https://doi.org/10.17531/ein.2020.2.15.
19. Lei G, Zhu J, Gou Y, Liu C, Ma B. A review of design optimization method for electrical machines. Energies 2017; 1962(10), https://doi.org/10.3390/en10121962.
20. Lewis M, Murray J. D. Modeling territoriality and wolf-deer interactions. Nature 1993; 366: 738 -740, https://doi.org/10.1038/366738a0.
21. Li Y, Yang R, Zhao X. Reactive power convex optimization of active distribution network based on improved grey wolf optimizer. Archives of Electrical Engineering 2020; 61,(1): 117 - 131.
22. Madadi A, Motlagh Mosheni A. Optimal control of DC motor using Grey Wolf optimizer algorithm. Technical Journal of Electrical Engineering and Applied Science 2014; 4(4): 373 - 379.
23. Marcic T. A short review of energy-efficient line-start motor design. Przegląd Elektrotechniczny 2011; 87 (3): 119 - 122.
24. Meach D L. Alpha statue dominance, and divisions of labor in wolf packs. Canadian Journal of Zoology 1999; 77: 1196 -1203, https://doi.org/10.1139/z99-099.
25. Mirjalili S, Mirjalili S. M, Lewis A. Grey wolf optimizer. Advances in Engineering Software 2014; 69: 46 - 61, https://doi.org/10.1016/j.advengsoft.2013.12.007.
26. Moussouni F, Brisset S, Brochet P. Comparison of two multi-agents ACO and PSO for optimization of a brushless DC wheel motor. Intelligent Computer Techniques in Applied Electromagnetic Systems 2008: 3 - 10, https://doi.org/10.1007/978-3-540-78490-6_1.
27. Mutluer M, Sahman A, Cunkas M. Heuristic optimization based on penalty approach for surface permanent magnet synchronous machines. Arabian Journal for Science and Engineering 2020; 45: 6751-6767, https://doi.org/10.1007/s13369-020-04689-y.
28. Nowak L, Knypiński Ł, Jędryczka C, Kowalski K. Decomposition of the compromise objective function in the permanent magnet synchronous motor optimization. COMPEL 2015; 34(2): 496 - 504, https://doi.org/10.1108/COMPEL-07-2014-0173.
29. Sarac V. Performance optimization of permanent magnet synchronous motor by cogging torque reduction, Journal of Electrical Engineering 2019; 70(3): 218 - 226, https://doi.org/10.2478/jee-2019-0030.
30. Shaari G, Tekbiyik-Ersoy N, Dagbasi M. The state of art in particle swarm optimization based unit commitment: a review. Processes 2019; 7(733), https://doi.org/10.3390/pr7100733.
31. Sorgdrager A J, Wang R, Grobler A J. Multiobjective design of line-start PM motors using the taguchi method. IEEE Transactions on Industrial Applications 2018; 54(5), https://doi.org/10.1109/TIA.2018.2834306.
32. Sun K, Wang G, Lu Y. Optimization method of bevel gear reliability based on genetic algorithm and discrete element. Eksploatacja i Niezawodnosc - Maintenance and Reliability 2019; 21(3): 186 - 196, https://doi.org/10.17531/ein.2019.2.2.
33. Wang Y, Filippini M, Bacco G, Bianchi N. Parametric design and optimization of magnetic gears with differential evolution method. IEEE Transactions on Industrial Applications 2019; 55(4): 3445-3452, https://doi.org/10.1109/TIA.2019.2901774.
34. Yang X S, Gandomi A H. Bat algorithm: a novel approach for global engineering optimization. Engineering Computations 2012; 29(5): 464 - 483, https://doi.org/10.1108/02644401211235834.
35. Yeniay Ö. Function methods for constrained optimization with genetic algorithms. Mathematical and Computational Application 2005; 10(1): 45 - 56, https://doi.org/10.3390/mca10010045.
36. Zang H, Zang S, Hapeshi K. A review of nature-inspired algorithm. Journal of Bionic Engineering 2010; 7: 232 - 237, https://doi.org/10.1016/S1672-6529(09)60240-7.
37. Zio E, Mellal M. System reliability-redundancy optimization with cold-standby strategy by an enhanced nest cuckoo optimization algorithm. Reliability Engineering & System Safety 2020; 201, https://doi.org/10.1016/j.ress.2020.106973.
38. Zhao M, Wang X, Yu J, Bi J, Xiao Y, Zhan J.. Optimization of construction duration and schedule robustness based on hybrid grey wolf optimizer with sine cosine algorithm. Energies 2020; 13(215), https://doi.org/10.3390/en13010215.
39. Zöhra B, Akar M, Eker M. Design of novel line-start synchronous motor rotor. Electronics 2019; 8(25), https://doi.org/10.3390/electronics8010025.